

Jets, Stickiness and Anomalous Transport

Xavier Leoncini

*Courant Institute of Mathematical Sciences, New York University, 251 Mercer St., New York, NY 10012, USA**

George M. Zaslavsky

*Courant Institute of Mathematical Sciences, New York University,
251 Mercer St., New York, NY 10012, USA[†] and*

Department of Physics, New York University, 2-4 Washington Place, New York, NY 10003, USA

Abstract

Dynamical and statistical properties of the vortex and passive particle advection in chaotic flows generated by four and sixteen point vortices are investigated. General transport properties of these flows are found anomalous and exhibit a superdiffusive behavior with typical second moment exponent $\mu \sim 1.75$. The origin of this anomaly is traced back to the presence of coherent structures within the flow, the vortex cores and the region far from where vortices are located. In the vicinity of these regions stickiness is observed and the motion of tracers is quasi-ballistic. The chaotic nature of the underlying flow dictates the choice for thorough analysis of transport properties. Passive tracer motion is analyzed by measuring the mutual relative evolution of two nearby tracers. Some tracers travel in each other vicinity for relatively large times. This is related to an hidden order for the tracers which we call jets. Jets are localized and found in sticky regions. Their structure is analyzed and found to be formed of a nested sets of jets within jets. The analysis of the jet trapping time statistics shows a quantitative agreement with the observed transport exponent.

I. INTRODUCTION

Transport phenomena can vary from electrons in conducting materials, pollutants in the oceans or atmosphere or even data across the Internet. Typically these phenomena are more often dealing with the transport of macroscopic scalar quantities such as temperature or density, in other words systems for which the access to actual microscopic information is beyond reasonable means and in some regards overwhelming if not useless. One of the first major steps towards a proper description of transport arose with the introduction of Fick's and Fourier's laws which describe respectively the evolution of the density or heat current. Assuming further simplifications both of these laws lead to the well known heat equation and the related diffusion coefficient. The introduction of the notion of Brownian motion and its associated probabilistic description allowed to link back this heat equation to the microscopic world, which then is pictured as a collection of random walkers. This may be a rather crude and oversimplified picture of the current problems related to transport, but still today most of this probabilistic spirit remains and in this sense the assumption of some underlying randomness is often made. On the other hand, when considering dynamical systems, the "microscopic" quantities are completely or almost completely deterministic and typically evolve with time in a ballistic or accelerated way. As a result there is a strong apparent dichotomy underlying the diffusive or ballistic nature of transport. This dichotomy being directly related to the properties of the underlying dynamics, and in a sense to whether or not the dynamics preserve or loose mem-

ory. This diffusive or ballistic nature of transport for a given system is usually inferred by the time evolution of the second moment of its characteristic distribution, namely $\sim t$ for a diffusive regime and $\sim t^2$ for the ballistic one. Nature is however not so reductive and for numerous systems the behavior $\sim t^\mu$ with $0 < \mu < 2$ or even more complicate, is observed: transport is so-called anomalous. These anomalous properties result from a subtle interplay of both the diffusive and ballistic behaviors and are linked to Levy-type processes and their generalizations [1]-[13].

In this paper we address the question of the motion of a passive tracer evolving in an unsteady incompressible two dimensional flow. The underlying problem is related to the transport and mixing in fluids, or more specifically, geophysical flows [14]-[20]. In order to tackle this problem and especially the anomalous features often observed in geophysical flows, our approach has been gradual and the present work follows from a series of papers [21]-[25], which consists of progressive successive steps of the investigations of problems of transport in two-dimensional flows from the dynamical point of view. The approach originates from the uncovering of the phenomenon of chaotic advection [26]-[34], that describes the possible chaotic nature of Lagrangian trajectories in a non chaotic velocity field and hence reflects a non-intuitive interplay between the Eulerian and Lagrangian perspective. The rise of chaos in these low dimensional systems allows to considerably enhance the mixing properties which would have else to rely on molecular diffusion. However the non-uniformity of the phase space and the presence of islands of regular motion within the stochastic sea has a considerable impact on the transport properties of such systems. The phenomenon of stickiness on the boundaries of the islands generates strong "memory effects" as a result of which transport becomes anomalous. In this case the rise of anomalous transport can be directly understood

*Electronic address: leoncini@cims.nyu.edu

†Electronic address: zaslav@cims.nyu.edu

by the underlying dynamics, and gives the means of a well defined probabilistic description [24]. However, typical geophysical flows can not in general be considered as low dimensional systems, hence one is tempted consider the method of two-dimensional turbulence (i.e as high-dimensional system from the dynamical stand point) by introducing some noise term in order to simplify the dynamics of tracers and obtain different properties of this ad hoc noise by comparing analytical estimates with experimental or numerical results.

The present approach tackles these problems from another perspective, namely a relatively simple model is chosen and a thorough analysis of the dynamics of tracers is performed. In other words, instead of introducing noise, we mask our ignorance by simplifying the actual system from the start and take a pure dynamical perspective of the problem. We believe that we may in this way shed some light on the kinetics which actually govern transport and hence complement the more traditional probabilistic description. To settle for a model we emphasize on another peculiarity of two-dimensional turbulent flows, namely the presence of the inverse energy cascade, which results in the emergence of coherent vortices, dominating the flow dynamics [35]-[41]. For these systems point vortices have been used with some success to approximate the dynamics of finite-sized vortices [42]-[44], as for instance in punctuated Hamiltonian models [41, 45, 46]. Moreover, point vortices have been recently used to describe exact unstationnary two-dimensional solution of the Navier-Stokes equation [47], we may thus also envision that the chaotic motion of the vortices shall reproduce to some extent the properties of a more realistic flow. It therefore seemed natural to consider a system of point vortices as our paradigm.

In the previously mentioned work, the advection in systems of three and four point vortices evolving on the plane has been extensively investigated [21]-[24]. Three point-vortex systems on the plane have the advantage of being an integrable system and often generate periodic flows (in co-rotating reference frame)[48]-[53]. This last property allows the use of Poincaré maps to investigate the phase space of passive tracers whose motion belongs to the class of Hamiltonian systems of 3/2 degree of freedom. A well-defined stochastic sea filled with various islands of regular motion is observed and among these are special islands also known as “vortex cores” surrounding each of the three vortices. Transport in these systems is found to be anomalous, and the exponent characterizing the second moment exhibit a universal value close to 3/2, in agreement with an analysis involving fractional kinetics [23, 24]. In this system, the origin of the anomalous properties and its multi-fractal nature is clearly linked to the existence of islands within the stochastic sea and the phenomenon of stickiness observed around them [23, 24]. The motion of N point vortices on the plane is generically chaotic for $N \geq 4$ [54]-[56]. The periodicity is then lost when considering a system of four vortices or more, but snapshots of the system have revealed the cores sur-

rounding vortices are a robust feature [57]-[58], the actual accessible phase space is in this sense non uniform and stickiness around these cores has been observed [25]. In order to find out if these properties remain for a large number of vortices, as well as if they may be at the origin of anomalous features of the transport properties of these systems, a thorough analysis is required.

In the following we investigate the advection properties of passive tracers in flows generated by respectively 4 and 16 identical vortices. In Section II, we recall briefly the dynamics of point vortices and of passive tracers. In Section III the dynamics of the system of 16 vortices is investigated, basic properties such as the time-averaged spatial distribution or minimal inter-vortex distance are computed numerically. We observe and describe a formation of pair and triplet of vortices, obtain statistics of pairing times in a power law tail, implying finite average of pairing times as well as strong non trivial memory effects. The measured pairing-time distribution exponent proves to be close to its proposed analytical estimate. In Section IV, we consider the motion of a passive tracer in a four vortex system and develop a new methodology for studying the relative evolution of two nearby “sticky” tracers using a notion of chaotic jet [59]. The distribution of trapping times within jets and the associated Lyapunov exponents are computed. The former exhibit a power-law tail. Chaotic jets are located and are directly linked to the sticking behavior of tracers, moreover their structure is analyzed and exhibit a nested set of jets within jets. The introduction of a “geometric” Lyapunov exponent allows to characterize independently each sticky zone. The method is then successfully applied to the system of sixteen vortices, leading to a possible dynamical mechanism of detecting coherent structures. In Section V, we consider transport properties of the 16 vortices as well as those of the tracers in both systems of 4 and 16 vortices. All are found to be anomalous with characteristic exponent $\mu \sim 1.8$, in good agreement with observed trapping times exponent and the kinetic theory discussed in [24].

II. VORTEX AND PASSIVE TRACER DYNAMICS

System of point vortices are exact solutions of the two-dimensional Euler equation

$$\frac{\partial \Omega}{\partial t} + [\Omega, \Psi] = 0 \quad (1)$$

$$\Delta \Psi = \Omega, \quad (2)$$

where Ω is the vorticity and Ψ is the stream function. The vortices describe the dynamics of the singular distribution of vorticity

$$\Omega(z, t) = \sum_{\alpha=1}^N k_{\alpha} \delta(z - z_{\alpha}(t)), \quad (3)$$

where z locates a position in the complex plane, $z_\alpha = x_\alpha + iy_\alpha$ is the complex coordinate of the vortex α , and k_α is its strength, in an ideal incompressible two-dimensional fluid. This system can be described by a stream function acting as a Hamiltonian of a system of N interacting particles (see for instance [60]), referred to as a system of N point vortices. The system's evolution writes

$$k_\alpha \dot{z}_\alpha = -2i \frac{\partial H}{\partial \bar{z}_\alpha}, \quad \dot{\bar{z}}_\alpha = 2i \frac{\partial H}{\partial (k_\alpha z_\alpha)}, \quad (\alpha = 1, \dots, N), \quad (4)$$

where the couple $(k_\alpha z_\alpha, \bar{z}_\alpha)$ are the conjugate variables of the Hamiltonian H . The nature of the interaction depends on the geometry of the domain occupied by fluid. For the case of an unbounded plane, the resulting complex velocity field $v(z, t)$ at position z and time t is given by the sum of the individual vortex contributions:

$$v(z, t) = \frac{1}{2\pi i} \sum_{\alpha=1}^N k_\alpha \frac{1}{\bar{z} - \bar{z}_\alpha(t)}. \quad (5)$$

and the Hamiltonian becomes

$$H = -\frac{1}{2\pi} \sum_{\alpha>\beta} k_\alpha k_\beta \ln |z_\alpha - z_\beta| \equiv -\frac{1}{4\pi} \ln \Lambda. \quad (6)$$

The translational and rotational invariance of the Hamiltonian H provides for the motion equations (4) three other conserved quantities, besides the energy,

$$Q + iP = \sum_{\alpha=1}^N k_\alpha z_\alpha, \quad L^2 = \sum_{\alpha=1}^N k_\alpha |z_\alpha|^2. \quad (7)$$

Among the different integrals of motion, there are three independent first integrals in involution: H , $Q^2 + P^2$ and L^2 ; consequently the motion of three vortices on the infinite plane is always integrable and chaos arises when $N \geq 4$ [50].

On the other hand, the evolution of a tracer is given by the advection equation

$$\dot{z} = v(z, t) \quad (8)$$

where $z(t)$ represent the position of the tracer at time t , and $v(z, t)$ is the velocity field (5). For a point vortex system, the velocity field is given by Eq. (5), and equation (8) can be rewritten in a Hamiltonian form:

$$\dot{z} = -2i \frac{\partial \Psi}{\partial \bar{z}}, \quad \dot{\bar{z}} = 2i \frac{\partial \Psi}{\partial z} \quad (9)$$

where the stream function

$$\Psi(z, \bar{z}, t) = -\frac{1}{2\pi} \sum_{\alpha=1}^4 k_\alpha \ln |z - z_\alpha(t)| \quad (10)$$

acts as a Hamiltonian. The stream function depends on time through the vortex coordinates $z_\alpha(t)$, implying a non-autonomous system.

In the following we focus on systems with $N = 4$ and $N = 16$ vortices. Due to chaotic nature of the evolutions we rely heavily on numerical simulations. The trajectories of the vortices as well as those of the passive tracers are integrated numerically using the fifth-order symplectic scheme described in [61] and which has already been successfully used in [21, 23, 24, 25].

III. 16-VORTEX SYSTEM FEATURES, PAIRING PROPERTIES AND SOME STATISTICS

A. Description of the system

We shall start by defining the system of 16 vortices which we will use to generate the flow advecting passive tracers. As we evolve from the 4 vortex system described in [25] to 16 vortices the phase space is considerably increased and due to the long range interaction

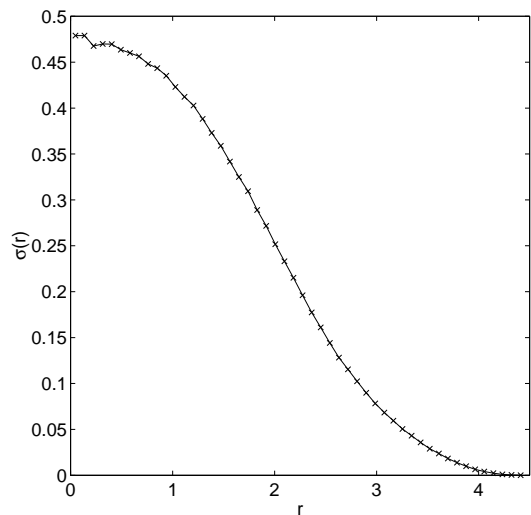


Figure 1: Spatial density distribution of the vortices obtained with one trajectory computed up to $t = 10^5$ (corresponding to $1.6 \cdot 10^6$ data points). Due to vortex indifferenciation (permutation symmetry) and the rotation invariance, the density depends only on r , *i.e.* on the distance from the center of vorticity, and it is identical for each individual vortex with the same r . We notice a bell shaped distribution which is reminiscent of the Lamb-Oseen vortex. Note that the non-uniformity does not necessarily imply non-ergodicity.

between vortices the energy does not behave as an extensive variable. However the constant L^2 defined in (7) seems to scale as r_{max}^3 , where r_{max} is the maximum distance reached between vortices, provided that the origin of our systems corresponds to $Q + iP = 0$ and the vortex strengths are all equal and the vortices have approximately a uniform distribution. In order to keep some coherence between the four vortex system and the sixteen vortex one, we chose to keep the average area occupied by each vortex approximatively constant. The switch from 4 to 16 vortices can then be thought of as increasing the

domain with non-zero vorticity while keeping the vorticity constant within the patch, in other words we choose not to concentrate nor to dilute vorticity while increasing the number of vortices. In this light we can write that the area occupied by the vortices is such that $r_{max}^2 \sim N$, and thus $L \sim N^{3/2}$, which leads to $L = 64$ for $N = 16$ and is our choice for L . The initial condition is chosen randomly within a disk, we choose such a configuration so that there is no vortices with close neighborhood to avoid any possible forced pairing. After that all position are rescaled to match the condition $L = 64$. The resulting simulation show that the vortices are evolving within a disk of radius ~ 4 (see Fig. 1), which corresponds to $r_{max}^2/N \sim 1$. We recall that for the four vortex system with $L = 4$, we have $r_{max}^2/N \sim 1$ too, and that the expression $L \sim N^{3/2}$ is not correct for only four vortices.

We can notice in Fig. 1, that the time averaged spatial distribution of the point vortices is not uniform, it has a bell shape which can remind us of an extended vortex such as the Lamb-Oseen one. The stationary distribution illustrated in Fig. 1 is a time average and in general it can not be associated with an extended stationary solution of the Euler equation (1). We shall not go into further details, but this non-uniformity by concentrating vortices in the center is likely to lead differences between the 4 and 16 vortex system, especially regarding the minimum inter-vortex distance and the resulting core size, which, as it will be seen later, are both be much smaller in the 16 vortex system than in the 4-vortex one.

We now move on to vortex pairing and pairing time distributions.

B. Minimum distance between vortices, vortex pairing and triplets

It has been found in [25] for a 4-vortex system that the pairing of vortices dramatically influences the trapping of tracers at the periphery of the vortex cores. Namely the pairing allows the sticky region around the cores to exchange trapped tracers, while “opening the door” for new tracers to be trapped or some to escape. Since the same behavior should occur with sixteen vortices, we decided to investigate the pairing behavior of the considered 16-vortex system. For this purpose we carried out a simulation up to $t = 10^5$, and checked the behavior of inter-vortex distances versus time. The results indicate that long time vortex pairing exists and one vortex pairing which lasts $\Delta t \sim 10^4$ is illustrated in Fig. 2. We also notice that during the pairing a triplet (a system of 3 bound vortices) is formed for about $\Delta t \sim 500$. The phenomenon of formations of triplets and pair of vortices concentrates vorticity in small regions of the plane (see Fig. 3) and in some sense is reminiscent of the inverse energy cascade observed in 2D turbulence. Since no quadruples are observed, we recall that both systems of 2 or 3 vortices are integrable, and may hence wonder whether the observation of triplets and pairs is just pure coincidence or

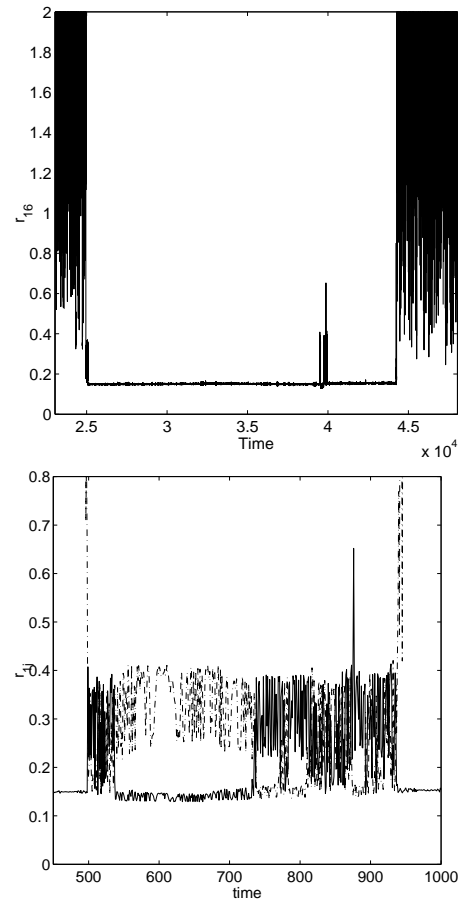


Figure 2: Observation of a very long pairing of two vortices: $\Delta t \approx 2 \cdot 10^4$ (upper plot). We notice a bump in the pairing around $t = 4 \cdot 10^4$. The analysis of this bump reveals the formation of a triplet of vortices (lower figure) which lasts about $\Delta t \approx 450$, which is still very large compared to typical time scales. In the upper plot the relative distance between vortex 1 and 6 is plotted versus time, while in the lower plot we added also the relative distance between vortex 1 and 16 (dashed line) for the time-length of the observed bump.

that the long memory effects associated with stickiness are intimately linked to this type of behavior. Namely, for passive tracers in the three vortex systems, the phenomenon of stickiness is associated with tracers that stay a “long time” in the vicinity of a island and mimic the regular trajectory of tracers trapped within the island. This notion was somewhat extended in [25], where the pairing behavior in the 4-vortex system was described as a sticking phenomenon to an object of lesser dimension than the whole phase space. However we speak about the pairing in the 4-vortex system as a reduction to an integrable 3-vortex system. It is therefore tempting to generalize this behavior as a sticking phenomenon to an object of lesser dimension than the actual phase space, but with some constraints. The subspace is reached by generating subsystems which integrability is a good approximate for a fairly long time. In this light, stickiness

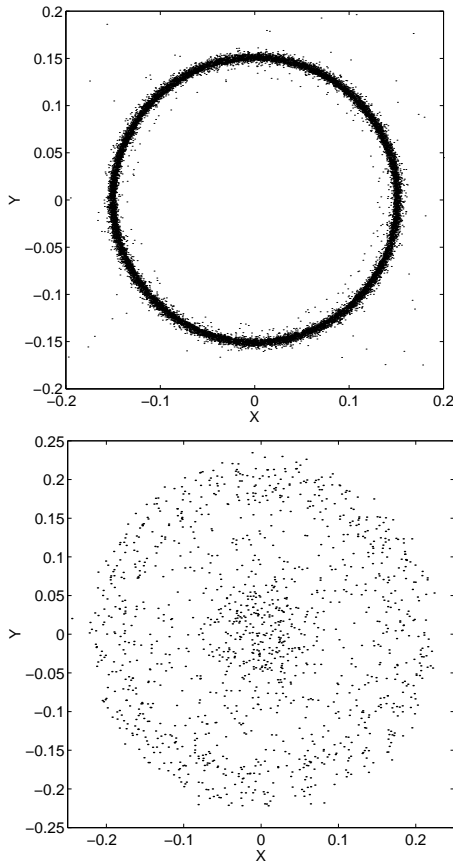


Figure 3: In this figure the relative positions of the vortices involved in the pairing, corresponding to Fig. 2, are plot. The upper plot shows the position of vortex 6 relative to vortex 1 versus time. The lower plot shows the positions of vortex 1, 6, 16 relative to their center of vorticity. In both cases we notice that the space occupied by the system has a typical radius of around 0.2 which is to be compared to an average area occupied by each vortices of ~ 1 .

would put some condition on the actual structure of potential clusters of vortices, for instance quadruples would be possible to encounter only if two out of the four vortices are involved in a pairing on a smaller scale, giving rise to a triplet on a larger scale. However we have not confirmed nor infirmed this scenario with the system of 16 vortices, and hence shall keep for now the simpler generalized notion of stickiness defined in [25, 62, 66]. In any case, both the triplet and pairing events described in Fig. 2 correspond to a sticking behavior, as the system remains a long time on a given subset of the phase space. For comparison we mention that a typical time of an eddy turnover used in [16], corresponds to a time of order $\Delta t \sim 1 - 5$.

Finally by detecting the pairing of vortices we were, at the same time, able to measure the minimum distance between vortices. It was suggested in [57] that the minimum distance can be a pretty good indicator of the double of the size of the vortex cores surrounding the vortices

[24, 25]. We found out that $\min(r_{ij}) \approx 0.13$ which implies that the core radius estimate r , given by a half of the minimum of the inter-vortex distance should be of the order $r \sim 0.065$.

C. Pairing time statistics

In the previously mentioned works [23, 24], it has been shown that the stickiness, providing long coherent motion, leads to anomalous transport properties and distributions with power law tails. We will show how the vortex pairing is related to the stickiness phenomenon and how it influences on the motion of passive tracers. Following the methodology and the results presented for 4 vortices in [25], we consider statistical data on pairing times for the 16-vortex system, using the previously run simulation of vortex motion up to time $t = 10^5$. The detection of pairing events is obtained with the same technique directly inspired from Fig. 2: a pairing occurs if for a given length of time two vortices stay close together. The results obtained for the four vortex system were independent on the arbitrary cutoffs chosen to characterize a pairing event, hence we chose the arbitrary time length to be $\delta t = 5$ (this value does not affect the behavior of large pairing time), and the distance from one vortex to another is such that $r_{ij} = |z_i - z_j| \leq 1$. To gather the statistics we proceed as was done in [25] and computed the the integrated probability $N(\tau)$ of pairings that last longer than a time τ

$$N(\tau) = N(T > \tau) \sim \int_{\tau}^{\infty} \rho(T) dT, \quad (11)$$

where $\rho(T)dT$ is the probability density of an event to last a time T . The results are shown in Fig. 4. The analysis of the distribution tail gives a power-law decay of $N(\tau) \sim \tau^{-\gamma_p+1}$ with the pairing exponent $\gamma_p \sim 2.68 \pm 0.1$ that confirms the non-negligible occurrence of long lasting pairings. The behavior of the probability density of pairing $\rho(\tau)$ lasting a time τ , is obtained from Eq. (11)

$$\rho(\tau) \sim \frac{dN}{d\tau} \sim \frac{1}{t^{\gamma_p}}. \quad (12)$$

This behavior provides a finite mean pairing time, but the second moment is infinite if the value of γ_p can be extrapolated. As suggested in the next section, pairing leads to one of the many form of stickiness, hence the pairing-times are to link to the trapping time within a sticky domain of phase space and parameters.

In the following subsection, we provide an estimate of γ_p .

D. Pairing exponent

The main idea used to estimate the value of the paring exponent γ_p follows the results presented in Refs.[67] and

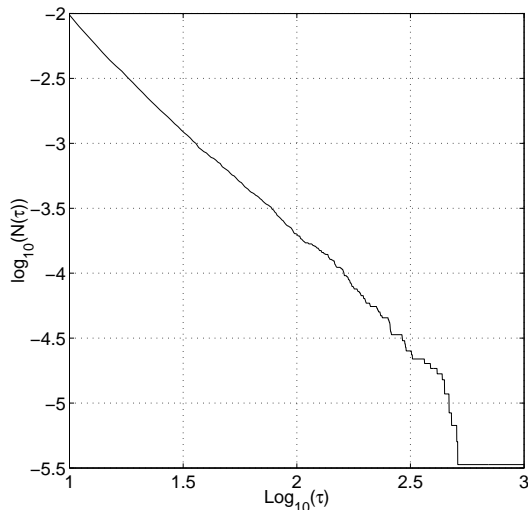


Figure 4: Distribution of integrated pairing times (see definition (11)) for the system of 16 vortices. We notice an algebraic time decay $N \sim \tau^{-\gamma_p+1}$ with $\gamma_p \approx 2.68$.

[24]. The idea revolves around the presence of an island of stability leading to ballistic or accelerator modes within the island. These islands appear in the stochastic sea as a result of a parabolic bifurcation [63] and correspond to the so-called tangled islands [64]. This is fairly general and it is reasonable to link the sticky phenomenon of vortex-pairing to the rise of an island in the stochastic sea, *i.e.* the formation of virtual potential well for the dynamics of a pair of vortices. Another way to validate this point of view comes from the pair perspective. While the pair exists an integrable system is formed which is perturbed by the flow generated by other vortices. To deal with the problem we use the general form of effective Hamiltonian proposed in [63] (see also [67] and [66]):

$$H_{eff} = b(\Delta P)^2 - a\Delta Q - V_3(\Delta Q), \quad (13)$$

where ΔP and ΔQ are respectively generalized momentum and generalized coordinate of the pair of vortices, the interaction potential V_3 is a third order polynomial and a, b are constants. The higher order terms in ΔQ can be neglected for the effective Hamiltonian.

Let us assume that the pairing corresponds to the occurrence of an island in the stochastic sea and that effective regular trajectories of the pair can be described by H_{eff} given in (13). This island has an elliptic point $\xi_e = (P_e, Q_e)$. Since the island has a finite size, a typical trajectory $\xi = (P, Q)$, located within the island corresponds to periodic or quasiperiodic dynamics and can be characterized by its relative coordinates $(\Delta Q, \Delta P) = \xi - \xi_e$. When the boundary of the island is reached, the values of the generalized coordinates $\xi^* = (P^*(t), Q^*(t))$ are such that the trajectory can access the whole stochastic sea, but cannot enter the island (the generalized phase space is two-dimensional).

The following steps are fairly formal (see also [66] and [24]). Let us consider a trajectory which is close to

the island's edge, which we monitor by the coordinates $(\delta P, \delta Q) = \xi - \xi^*$. A small perturbation is then likely to allow the trajectory to “escape” from the island vicinity and consequently to destroy the vortex pair. The phase volume of the escaping trajectory writes:

$$\delta\Gamma = \delta P \delta Q, \quad (14)$$

where $\delta P, \delta Q$ are the values of the escaping trajectory. Since the trajectory is close to the islands edge (inflexion point), we can estimate from Eq. (13)

$$\delta P \sim \delta Q^{\frac{3}{2}}, \quad (15)$$

where we have assumed $V_3(Q) \sim Q^3$. Using this last expression (15), we obtain for (14)

$$\delta\Gamma = \delta Q^{\frac{3}{2}} \delta Q \sim \delta Q^{\frac{5}{2}}. \quad (16)$$

Due to the periodic or quasiperiodic nature of the trajectories within the island, any sticking trajectory (in its neighborhood) experiences a ballistic type behavior, which translates into $\delta Q \sim t$, *i.e.*

$$\delta\Gamma \sim t^{\frac{5}{2}}. \quad (17)$$

The probability density to escape the island vicinity after being in its neighborhood for a time t (*i.e.* time-length of the pairing) within an interval dt is then

$$\rho(t) \propto \frac{1}{\delta\Gamma(t)} \sim t^{-\frac{5}{2}}, \quad (18)$$

this results gives us directly the estimate of the exponent $\gamma_p \approx 5/2$, which is very close to the observed value 2.7 ± 0.1 .

This estimate is not rigorous and essentially based on phenomenological grounds, however we believe it provides a good insight on the origin of different characteristic exponents of trapping time distributions. We now remind the reader that for the 4-vortex system the value observed in [25] for characteristic exponent was $\gamma_p \approx 7/2$. This value was explained in a very similar way as what has just been developed before but one more generalized spatial coordinates was introduced. A 4-vortex system is non generic. Indeed as a pair is formed, the whole system becomes a quasi 3-vortex system, the pair acting as one vortex with increased strength, hence the remaining system is itself integrable. In this light, when switching to the idealized generalized variables (P, Q) , we should consider more degrees of freedom to describe the pair of vortices, namely

$$H_{eff} = c_1(\Delta P_1)^2 + c_2(\Delta P_2)^2 + V_3(\Delta Q_1, \Delta Q_2). \quad (19)$$

The Hamiltonian (19) is in general non-integral, and the appearance of an island of stability adds an additional constraint or integral of motion to the system governed by (19). Taking this constraint into account the Hamiltonian (19) can be transformed into

$$H_{eff} = c(\Delta P)^2 + V_3(\Delta Q_1, \Delta Q_2), \quad (20)$$

where ΔP is a new (collective) momentum. The corresponding phase volume of the escaping trajectories gives in analogy to (14):

$$\delta\Gamma = \delta P \delta Q_1 \delta Q_2 \sim \delta Q^{5/2}, \quad \} (Q \sim \delta Q_{1,2}) \quad (21)$$

This leads to the estimate of $\gamma_p \approx 7/2$, in contrary to Eq. (18) with $\gamma_p \approx 5/2$. Note that the extra spatial generalized coordinate introduced in [25], can also be thought as a consequence of having two different coexisting quasi-integrable subsystem described by different actions, but however linked as they cannot “live” without one-another.

We have now a sufficient knowledge of the dynamics of the vortex systems, and move on to the behavior of passive tracers generated by these flows.

IV. JETS

A. Definitions

As it was previously mentioned, the motion of point vortices is chaotic for both systems of four or sixteen vortices but the use of Poincare maps in these cases is impossible in contrary to [21, 23, 24]. To investigate the anomalous transport properties from the first principles it is crucial to define a proper diagnostic which will be able to capture some singular properties of the dynamics that are clues of the origin of the anomalous transport of passive tracers.

For the system of 4 point vortices, successive snapshots have shown that passive tracers can stick on the boundaries of cores and jump from one core to another core or escape from the core due to their perturbations. The fact that a tracer is able to escape from a core means that the surrounding regions of the cores are connected to the region of strong chaos. The results presented in [25] indicate that these regions mix poorly with the region of strong chaos. One way to track this phenomenon is to use Finite-Time Lyapunov exponents (FTLE) and to eliminate domains of small values of the FTLE [58, 69, 70]. Once these exponents are measured from tracers’ trajectories whose initial conditions are covering the plane, a scalar field distributed within the space of initial conditions is obtained and the two dimensional plot of the scalar field reveals regions of vanishing FTLE, namely the cores surrounding the vortices and the far field region. The cores are thus regions of small FTLE, meaning that two nearby trajectories are bound together for long times, and this despite the core’s chaotic motion. These properties reveal typically a sharp change of the tracers dynamics as it crosses from the region of strong chaos to the core. This property is directly linked to the method described in in [68], which determines from a Lagrangian perspective the border of coherent structures in a turbulent flow. Namely, the method consists in computing a scalar field (typically FTLE’s) and extract the coherent structures by finding the spatial extrema of this

scalar field. The difficulties with these types of approach resides in the definition of the Lyapunov exponent

$$\sigma_L = \lim_{r(0) \rightarrow 0} \lim_{\tau \rightarrow \infty} \frac{1}{\tau} \ln \frac{r(\tau)}{r_0}, \quad (22)$$

where r_0 is the initial separation between two nearby trajectories and $r(\tau)$ is the separation at time τ . Indeed, the definition (22) introduces an arbitrary choice of two free parameters when computing FTLE, namely the initial separation between two different trajectories r_0 and the time interval τ within which they are computed. Moreover FTLE are not unique for a given trajectory which induces also a dependence on initial conditions x_0 , as well as time if the system is not autonomous. In the following we shall note FTLE as σ_L , but shall keep in mind that $\sigma_L = \sigma_L(\tau, r_0, x_0, t)$.

One problem that may arise when computing these exponents is related to the behavior of $r(t)$. For instance in the case of a system of four identical point vortices, the motion of tracers is more or less confined within a finite sized region and $r(t)$ has an upper boundary $R(t)$ which may be dependent on time if radial diffusion occurs, and no matter what initial distance r_0 and initial position x_0 , $\sigma_L \rightarrow 0$ as $\tau \rightarrow \infty$. This example is rather extreme and exaggerated as the results presented in [58] are able to capture the structure of the space of initial conditions, but we believe it illustrates clearly one problem encountered when using FTLE, namely that $r(t)$ is dependent on possible scales of the physical nature of the system. It is likely that $r(t)$ is not always smooth growing function of time on the scale of an arbitrary time τ and jumps between different spatial scales with a potential physical meaning which may get averaged with time. We can anticipate that this may be especially the case when different regions of small (if not zero) Lyapunov exponents are present in the system.

In the previous discussion it appears that FTLE are overall giving us good results in detecting coherent structures and regions of low chaos, but may also hide by averaging out a useful information as a result of a lack of capturing specific scales. In the following we propose an alternative diagnostic which is greatly inspired from typical FTLE but has the advantage of clearing out some of its shortcomings. Namely, FTLE is a straightforward approximation of the definition (22) of the Lyapunov exponent which is inherently nonlocal. In other words a Lyapunov exponent measures the “averaged” exponential divergence of two nearby trajectories, and assuming the system is ergodic it measures a degree of “chaoticity” of the whole dynamics of the considered system. This non-locality property may create serious difficulties in the interpretation of the results when the truncated characteristics of the dynamics has been used while for the considered time interval the ergodic theorem may not work (see more discussion in [[59]).

One possible way to circumvent this problem can be identified by the following remarks. We are most of the time dealing with only a finite portion of a trajectory (fi-

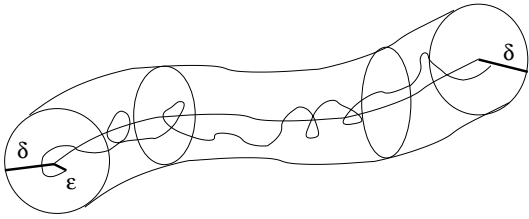


Figure 5: A tracer and a ghost are used to define a jet.

nite time) and only have a finite spatial resolution of these pieces of trajectories which is typically much smaller than the actual scales we are interested in. In this more practical situation, we are facing a “coarse grained” phase space, and each point is actually a ball from which infinitely many real trajectories can depart. Given this facts we can imagine that two nearby real trajectories diverge exponentially for a while but then get closer again without actually leaving the ball, a process which may happen over and over in the case of stickiness. From the “coarse grained” perspective those two real trajectories are identical. We then can infer that there exists bunch of nearby trajectories which may remain within the ball for a given time, giving rise to what is called a *jet* [59], and can be understood as a region of regular motion for our scale of interest. We are then mostly interested on the chaotic properties of the system from the ball scale and up and dismay any chaotic motion which may occur within the jet. The stickiness to a randomly moving and not well determined in phase space coherent structure imposes existence of jets, while the opposite may not be the case.

To actually measure the jets properties of the system, we use the following strategy. Let us consider a given trajectory $\mathbf{r}(t)$ evolving within the phase space. For each instant t , we consider a ball $B(\mathbf{r}(t), \delta)$ of radius δ centered on our reference trajectory. We then start a number of trajectories within the ball at a given time, and measure the time it actually takes them to escape the ball. Depending on how fast trajectories are escaping the ball we should then be able to identify if the reference trajectory is moving within a regular jet or is in a region of strong chaos.

B. Statistical Results

From the numerical point of view we first consider the velocity field generated by the chaotic motion of four point vortices and proceed as follows: given an initial condition of a tracer, two “ghost” particles are placed in its neighborhood, at a distance $\epsilon = 10^{-6}$, more specifically we placed one ghost along the tracer speed and the other one on the orthogonal direction, but this positioning should not affect the results. Then for each of the ghost particles, once each reaches a distance $\delta = 0.03$ (the radius of our ball) from the tracer, the time interval

Δt and the distance traveled Δs are recorded. For simplicity two new ghost particles are placed within the ball once both have escaped, while the old ones are discarded. One of the main difficulties in using this type of diagnostic relies in the fact that data acquisition is a priori not linear in time nor space and necessitates a careful choice for the values of ϵ and δ . Note that the value chosen for δ is small even compared to the minimum inter-vortex distance. However, using the definition (22) we can compute a different type of FTLE, which we define as follows:

$$\sigma_L = \frac{1}{\Delta t} \ln \frac{\delta}{\epsilon}, \quad \sigma_D = \frac{1}{\Delta s} \ln \frac{\delta}{\epsilon}, \quad (23)$$

where contrary to the typical definitions the value of the logarithm is fixed and Δt or Δs are the variables. These exponent are very similar to the notion of Finite Size Lyapunov Exponent (FSLE) considered in [71], however we do not perform averages over different scales and keep the whole distribution function. We computed these exponents for the flow generated by four vortices, with the same initial condition as the one used in [25]. The data are obtained using the trajectories of 4 different tracers initially placed in the region of strong chaos and advected by the chaotic flow generated by the motion of the 4 point vortices of equal strength. The time of the simulation is $5 \cdot 10^6$, the time step is 0.05, which leads to statistics computed using $\sim 3 \cdot 10^5$ data points. The results of the

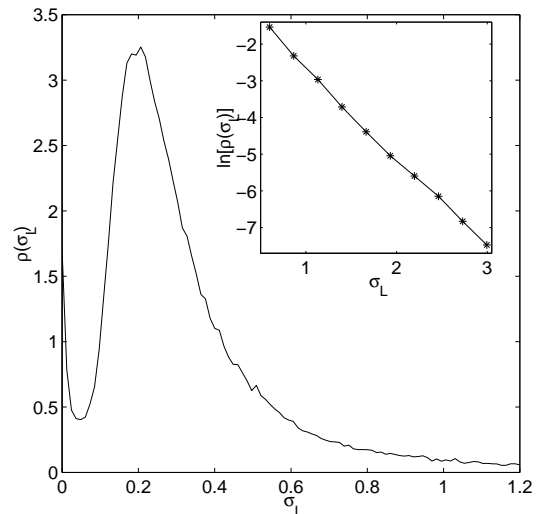


Figure 6: Distribution of time Lyapunov exponents σ_L (see Eq. (23)). We notice an exponential decay for high exponents. $\rho(\sigma_L) \sim \exp(-\sigma_L/\sigma_{L0})$ with $\sigma_{L0} \approx 0.4$. We can notice a minimum around $\sigma_L \approx 0.05$. The observed accumulation near 0 results from the existence of long lived jets. The local minimum gives an estimate of the minimum typical time interval corresponding to a jet: $\Delta t_{min} \approx 206$. Data are obtained with 4 different trajectories computed up to $t = 5 \cdot 10^6$ leading to 328.220 records.

measured σ_L are illustrated in Fig. 6. One can notice in this plot two different types of behavior.

First, the large FTLE decay exponentially with a characteristic exponent $\sigma_{L_0} \approx 0.4$, which is not a surprise since the speed of tracers is bounded. Hence even if the tracer and the ghost are going in opposite direction, it will always take them a finite time to escape from the ball, thus an expected maximum value for σ_L . Regarding the exponential decay behavior before reaching this maximum value, we can suspect it is directly related to the way the data is acquired; indeed we remind the reader that the acquisition is a priori nonlinear in time, and that we are in fact measuring escape times from a given moving region of the phase space, and since this behavior is related to the large FTLE's, we are just observing the exponential growth of the coarse grained volume.

The second behavior is, from the point of view of anomalous transport, more interesting. The local minimum for small FTLE can be seen in the probability density of σ_L as a crossover from the erratic chaotic motion of tracer within the chaotic region, to its motion within a quasi-regular jet. Indeed if the tracer is within jet, the ghosts are nevertheless expected to escape from the tracers vicinity but with trapping times exhibiting a power-law decay, therefore if the passive tracer is evolving within a jet for a long time, we should expect an accumulations of events corresponding to ghosts leaving the surrounding ball. This hypothesis is confirmed in Fig. 7, where the distribution of trapping times is plotted. The log-log plot clearly shows the power-law decay of the trapping times, with typical exponent $\gamma = 2.82$.

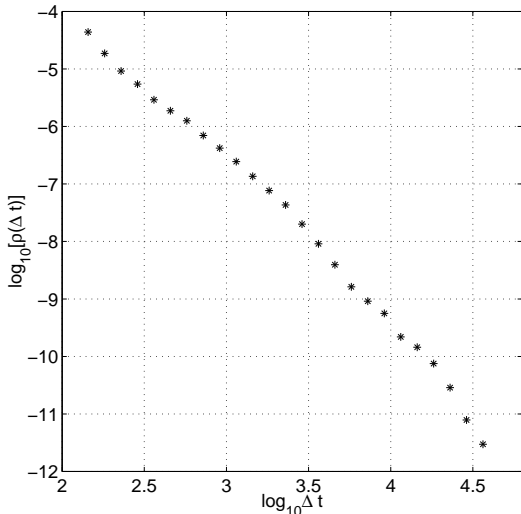


Figure 7: Tail of the distribution of time intervals Δt . We notice a power-law decay, with some oscillations. Typical exponent is $\rho(t) \sim t^{-\gamma}$ with $\gamma \approx 2.823$. Data is obtained with 4 different trajectories computed up to $t = 5.10^6$ leading to 328.220 records.

We shall now discuss the reason why another Lyapunov exponent σ_D was introduced in (23). By its definition σ_D measures how much two trajectories diverge depending on how much we travel along them, it is then inherently

time independent and can be seen as a pure geometric property of a trajectory or, from another point of view, time is locally rescaled depending on the local speed, so that the speed along the trajectory is constant and equal to one. The plot of the distribution of σ_D gives the same picture as the one obtained for σ_L in Fig. 6, with an exponential decay and a local minimum $\sigma_{D^*} \sim 0.03$ near zero, which also can be used as a criterion for identifying a coherent jet. We may argue that since the speed is bounded and almost everywhere non zero, the use of σ_D is redundant and therefore futile. Nevertheless from a practical point of view, the interval of possible speed is rather large; for instance in the case of the 4 vortex system, the core has a typical radius of 0.2 while the outer region corresponds to radii of around 4, we can thus expect an order of magnitude between the different speeds within the region of strong chaos and the outer region, moreover we can expect an increase of the range as we increase the number of vortices. It then becomes obvious that by measuring σ_L we are biased towards jets occurring in the outer region, while by using σ_D these dynamical differences are erased and only the actual topology of the vicinity of a trajectory matters. Hence when using σ_{D^*} to characterize a jet in a small simulation we obtained for the distribution of characteristic speeds the histogram plotted in Fig. 8, where it clearly shows that

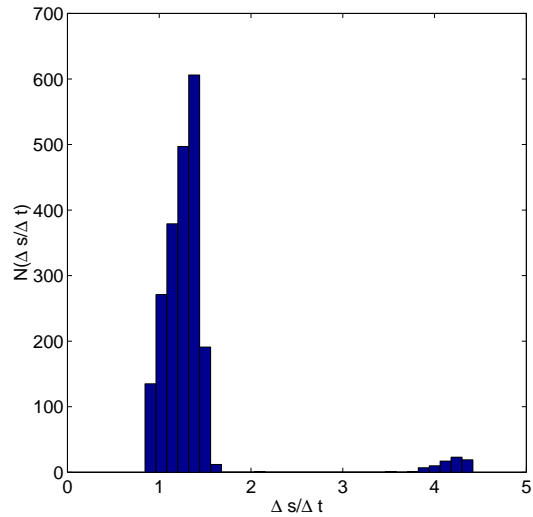


Figure 8: Distribution of the averaged speed of the tracer, for the data corresponding to $\sigma_D < 0.03$. We notice two regimes, the regime of fast speed corresponds to stickiness to the core. Note that if instead we use σ_L as a reference most of the fast particles lie after the local minimum in the distribution and mostly only one regime seems to be present.

actual fast jets exists, while if we had used only σ_L only a few fast jets are detected. In this light it seems that σ_{D^*} is a good candidate to identify a jet, while its averaged speed σ_L/σ_D gives a more refined idea on the nature of the jet.

C. Jets pictures

Given the previous results we shall now have a closer look at those jets. Namely, in the previous sections we defined what we considered a jet, computed statistics on them and were able with the results to obtain a threshold for which a jet can be considered regular. We just then have to put these results in application. Let us initialize a tracer in the region of strong chaos, but not in the vicinity of any vortex to avoid any trapping within a core. We can let the tracer evolve with its two ghosts nearby, once the threshold given by σ_D^* is reached (ghosts are still within the ball for a given length traveled) we know that the measured σ_D will be such that $\sigma_D < \sigma_D^*$, hence we are currently within what we considered a regular jet, we then just have to record the position of the tracer and vortices until ghosts have escaped. In this way we are able to locate the tracer for given length of time while it evolves within the jet. In fact we shall be even more picky, namely we know from Fig. 8, that the majority of jets correspond to slow motion, which when plotted corresponds to the tracer being in the far field region and simply rotating around the center of vorticity, hence to avoid recording the position of these events we can also use the averaged speed σ_L/σ_D and record only the jets corresponding to fast motion.

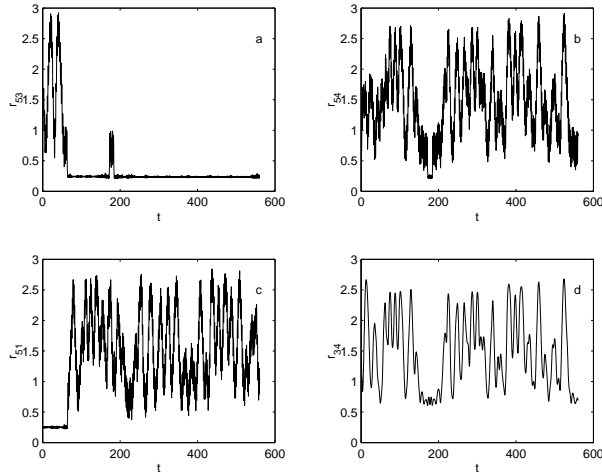


Figure 9: Plots of relative distance for an identified jet within the “strong chaos” area whose $\Delta t \approx 560$. Plots a,b,c: distances between the passive tracer and respectively vortex 3,4,1 versus time (the tracer is referred as particle 5). Plot d, distance between vortex 3 and 4 versus time. We notice that for this jet the passive tracer sticks to vortex cores. It can jump from core to core as vortex are pairing but is always sticking to one core.

The analysis of the portion of a detected single fast jet is illustrated in Figs. 9 and 10. This jet corresponds to a trapping time of the ghosts $\Delta t \approx 560$. Since we suspected that a jet would be located within the sticky zones surrounding the vortex cores, we plotted in Fig. 9 (a), (b), and (c) the distances between the tracer and

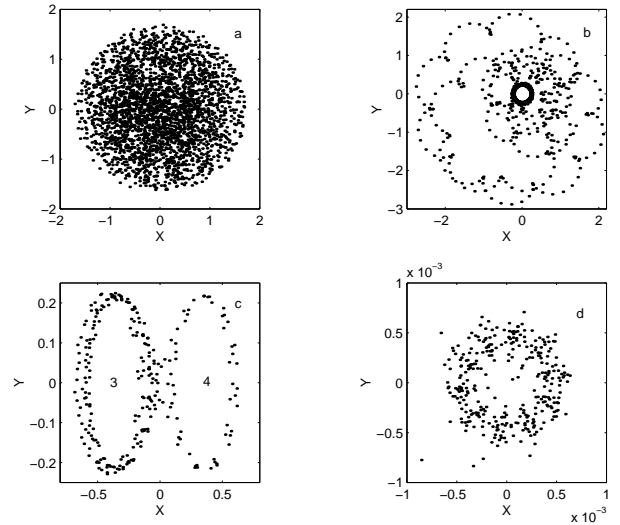


Figure 10: Plots of tracer’s positions for different times for an identified jet within the “strong chaos” area whose $\Delta t \approx 560$. Plot a, position in the absolute reference frame (it looks random!). Plot b, relative position of the tracer with respect to vortex 3 (see Fig. 9), we observe the sticking habits of the tracer. Plot c, relative position of the tracer with respect to the pair formed by vortex 3 and 4, during the pairing ($153 < t < 205$, see Fig. 9). Plot d, relative position of the ghost with respect to the tracer during the first part of the jet when tracer is sticking to vortex 1.

the vortices versus time, and it is rather clear that the tracer is always in the vicinity of a vortex during the jet, moreover we also notice that during its evolution the tracer jumps from one vortex to another: first the tracer was close to vortex 1, then it jumps to the vortex 3, then to vortex 4 and back to vortex 3. This results is consistent with the observations made in [25] that the sticky zone is the reunion of the surrounding of all vortices. The possibility of the formation of a pair of two bound vortices as well as the role of these pairings allowing tracers to jump between vortices as well as trapping (freeing) them within (from) sticking zones described in [25], lead us to assume that a pairing was the cause of the odd behavior of the tracer. This origin is confirmed in Fig 9 (d), the distance between the two concerned vortices is plotted and a pairing of the two vortices is observed for the time interval $150 < t < 200$.

In Fig. 10, the actual history of the jets is plotted in various reference frames. In the first figure 10 (a), we just plotted the absolute position of the tracer while it evolves in the jet, which clearly exhibits the difficulty of seeing any order. In the second figure 10 (b) the position of the tracer is plotted in the reference frame which is moving with vortex 3 (The one with whom the tracers spends most of its time as seen in Fig. 9 (a)), and the sticking behavior of the tracer during the jets becomes more clear. In 10 (c), we plotted the position of the tracer during the pairing of the vortices 3-4 observed in Fig 9 (d) in the reference frame whose origin is the center of vorticity of

the pair and which rotates such that the vortices are stuck oscillating in the x-direction. The double jump from one vortex back and forth and the exchange between cores is hence illustrated.

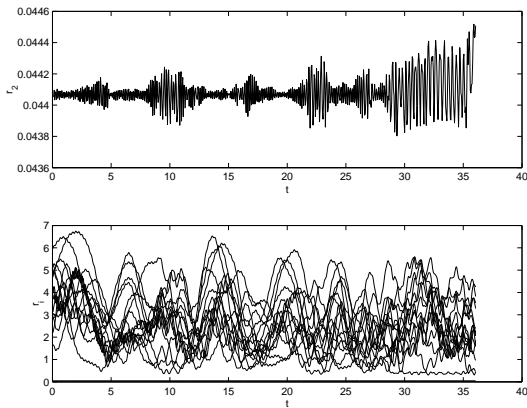


Figure 11: Distance between the tracer and vortices for a coherent jets detected in the system of 16 vortices. In the upper plot the distance relative to vortex 2 is plotted, while on the bottom there are the relative distances to all vortices. We notice towards the end of the jet that while the fluctuations of r_2 increase a pairing occurs between vortex 2 and another one. This is illustrated by the presence of another vortex nearby the tracer at the end of the jet.

These visualization of the location of the jets have confirmed the results already illustrated in [25] that the boundaries of the core exhibit the stickiness. However we would like to emphasize on the fact that in the present case, this property of the system has been diagnosed with the use of coherent jets, in other word by analyzing the relative evolution of two nearby trajectories within a specific scale (phase space ball). In this sense the method used is rather general, while in [25] a more detailed knowledge of the system was necessary to capture its “hidden order”. To test even further the method, we decided to apply it to the system of 16 vortices considered in section III. Given the previously obtained threshold for 4 vortices, we skipped the analysis of the distributions of σ_L , σ_D , and used the similar values to attempt the detection of a fast jet in the flow generated by 16 vortices. A jet is effectively detected and is illustrated in Fig. 11, meaning that the method is relatively robust since in this 16 vortex system the cores are much smaller. In this last figure we can notice that a pairing between two vortices is the cause of the end of the jet, but this may not be the real end of the jet; both ghosts have escaped but they may have jumped on the other core, while the tracer is still sticking or vice versa, hence we shall propose in a following paragraph some possible enhancements to the currently employed method. Besides this, we also get from Fig. 11 the actual size of the core, which is typically $r \sim 0.044$ and is within a reasonable range from the estimate given by half the minimum distance reached between vortices $\min(r_{ij})/2 \sim 0.06$, a fact which was also

observed for 3 and 4-vortex systems [24, 25].

In the next section we will consider a little further the notion of the jets as coherent structure.

D. Jets structure analysis

In the previous section we were able to characterize that a given tracer was evolving within what we called a jet, once a given threshold σ_D^* for the measured σ_D was reached, and then able to visualize the jet by recording the tracer’s position. In the meantime, why not also

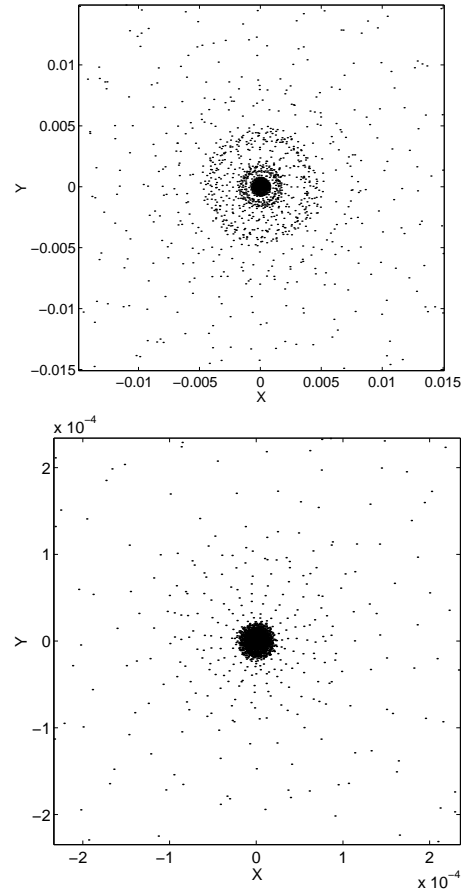


Figure 12: Relative evolution of a ghost within a long lived jets located in the far field region of the flow generated by four vortices. The lower plot is a centered zoom of the upper one (see the scales). The distribution within the jets is clearly not uniform suggesting a possible order organized as “matroschkas” (a nested set of jets with increasing radii).

record the positions of the ghosts, we should be then able to gather some information about the inner structure of the jet while practically it should incur a very little numerical overload besides maybe the need for more storage space.

A first plot of the evolution of a relative ghost position with respect to the tracer’s position is plotted in Fig 10 (d), where we only considered the first portion of the jet,

when the tracer is sticking to vortex 1. One can see some structure or skeleton within the ball. In order to confirm this possibility we looked for a longer lived jet, which for the 4 vortex case was easier to find in the far field region. Plots of such a long lived jet are presented in Fig. 12, where we effectively see a fine structure within the jet, which seems to be formed of a hierarchy of circular (tubular) jets within jets. Wondering if these features

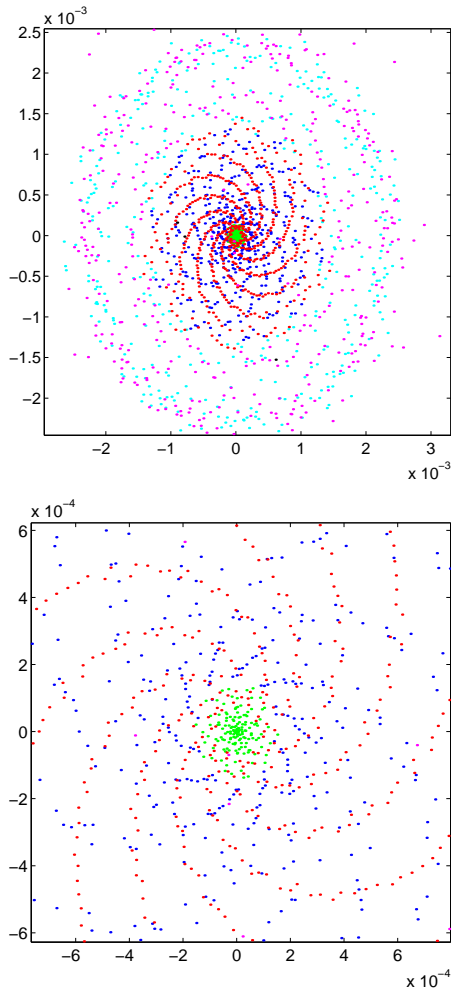


Figure 13: Jet structure for a long lived jet located in the region of strong chaos for a system of 16 vortices. The lower figure is a zoom of the upper one corresponding to a magnification of an order of magnitude. The colors are characterizing different moments of the life of the jet corresponding to approximately equal time intervals. They chronologically range as cyan<blue<green<red<magenta. We see a similar structure of jets within jets as observed in Fig. 12, and ghosts spiraling back and forth between them.

were general or specific to these 4 vortex systems, we decided to consider the fast jet illustrated in Fig.11 and check its structure. The results are plotted in Fig. 13, where the relative position of the ghost is colored differently for different time periods of the life of the jets. We can see that effectively the nested set of jets within jets

remains, and that the ghosts is also spiraling back and forth in between. This figure is also informative in the sense that we actually see the ghost going back very close to the tracer. In other words, the area characterized by the green points in Fig. 13 does not correspond to the beginning of the jet and therefore is not an artifact of having initially placed the ghost in the vicinity of the tracer.

We shall close this subsection with a final remark on this “matroschka” structure of the jets. Namely, this nested structure suggests that for each identified jet we can define a suite (r_n) , such that r_n is a decreasing function of n with $r_n \rightarrow 0$ and $n \rightarrow \infty$ and r_0 is for instance determined by the largest tube (jet) seen in Fig. 12 or Fig. 13. To each subset n we can assign a distribution of trapping time $\rho_n(\tau)$ as well as a transit time t_n (or a distribution) associated with the tracer spiraling from one subset n to one of its two neighbors $n-1$ or $n+1$. In this light depending on the transport properties of the whole system are likely to depend of the distributions $\rho_n(\tau)$ and the ratio r_n/r_{n+1} , and for instance if we have in the limit $n \rightarrow \infty$ both $r_n/r_{n+1} \rightarrow r_\infty$ and $\rho_n(\tau) \rightarrow \rho_\infty(\tau)$, the FSLE become effectively independent of scale within the jet. This hierarchical structure is also reminiscent of the discrete renormalization group, and hence we can speculate that log-periodic oscillation described in [72] may be observed.

V. TRANSPORT PROPERTIES

A. Definitions

For the considered case, all vortices have positive strength and therefore are moving within a finite domain. It is important to define what quantities will be measured to characterize the transport properties of the system. There has been evidence in [58] of radial diffusion, but the diffusion coefficient D is vanishing as $R \rightarrow \infty$ with typical behavior $D \sim 1/R^6$. In the case of more than four vortices we can still expect a similar type of behavior. However the far field region is of little interest when one want to address the transport properties of typical geophysical flows since the most relevant is the region being accessible to the vortices, *i.e* also called the region of “strong chaos”. In fact the same problem was faced when considering system of three point vortices. For these particular systems the vortex motion is integrable, which has for consequence to restrict the accessible domain of tracers within a finite region surrounded by a KAM curve. The way around this problem was then to measure how many times a tracer rotates around the origin, in other words measure the diffusion along an angular direction. However even though suitable, this solution may face some criticisms due to the singularity present at the origin. In this article we consider tracer transport in the way already used with some success in [24]. Namely the arclength $s(t)$ of the path traveled by

an individual tracer up to a time t , which writes

$$s_i(t) = \int_0^t v_i(t') dt', \quad (24)$$

where $v_i(t')$ is the absolute speed of the particle i at time t' . One advantage of this quantity is that it is independent of the coordinate system and as such we can expect to infer intrinsic properties of the dynamics. The main observable characteristics will be moments of the distance $s(t)$ defined in (24):

$$M_q = \langle |s_i(t) - \langle s_i(t) \rangle|^q \rangle, \quad (25)$$

where i corresponds either to the i -th vortex or a tracer in the field of 4 or 16 vortices. The averaging operator $\langle \dots \rangle$ needs a special comment. Expecting anomalous transport one should be ready to have infinite moments starting from $q \geq q_0$. Particularly it can be $q_0 = 2$. The value of q will vary from 0 to 8. To avoid any difficulty with infinite moments we consider truncated distribution function

$$\rho_{tr}(s_i) = 0, \quad s_i > s_i^*. \quad (26)$$

The condition (26) was discussed in details in [73] to satisfy the physical restriction of a finite velocity. This condition put some constraints on the maximum value q^* of q corresponding to the maximum time t^* , beyond which the moments are basically monitoring the population of almost ballistic trajectories.

Up to the mentioned constraints, we will always consider the operation of averaging to be performed over truncated distributions. In this perspective all moments are finite and one can expect

$$M_q = \langle |s_i(t) - \langle s_i(t) \rangle|^q \rangle \sim D_q t^{\mu(q)}, \quad (27)$$

with, generally, $\mu(q) \neq q/2$ as one would expect from normal diffusion. The nonlinear dependence of $\mu(q)$ means multifractality of the transport. Some authors use the notion of weak ($\mu(q) = \text{const} \cdot q$) and strong ($\mu(q) \neq \text{const} \cdot q$) anomalous diffusion [69, 70] or strong and weak self-similarity [74]. For more information on the appearance of multi-fractal kinetics and related transport see [75, 76].

B. Vortex transport properties in 16 vortex system

Due to the low dimensionality of a system of 4 point vortices, no typical transport behavior has been measured, but there is an analysis of the phase space topology and Poincare sections [25]. The results for 16 vortices were computed by using a number of different “equivalent” initial conditions. Such different trajectories were obtained by letting a given initial condition evolve and record the positions of the vortices at different times with a given accuracy (typically 10^{-5}), while making sure no vortices were initially involved in pairings. The strong

chaoticity of the system leads very rapidly to different trajectories while this choice of initial conditions let us keep the constant of motions within a relative small error. The transport properties are then obtained by averaging over all vortices as well as over different sets of trajectories that correspond to our specific arbitrary choice of the constants of motion. The results are presented in Fig. 14, where the exponent characterizing the long

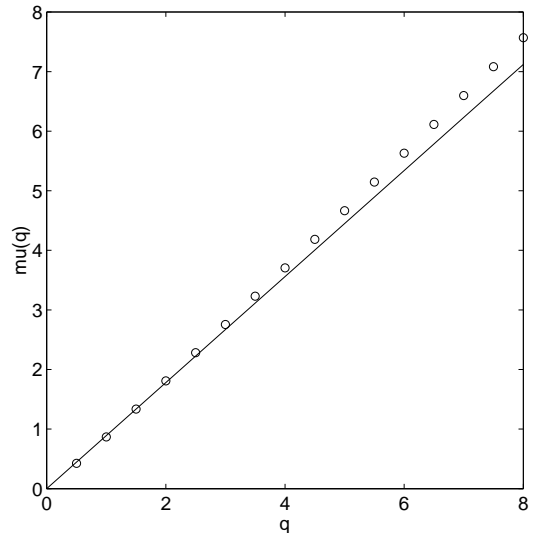


Figure 14: Large-time behavior for the different moments $\langle |s(t) - \langle s(t) \rangle|^q \rangle \sim t^{\mu(q)}$ for the flow of 16 point vortices, with $\mu(2) \approx 1.80$ corresponding to a superdiffusive regime.

time power law behavior of different moments is plotted versus moment order. The actual value of the second moment which is typically used to characterize the transport properties, is measured to be $\mu(2) \approx 1.80$ and indicates a strong superdiffusive behavior of the vortex subsystem. This behavior can be linked to the pairing of vortices which induces a strong quasi-ballistic dynamics of both vortices of the pair. Indeed let us compare the exponent $\gamma \approx 2.68$ characterizing the distribution of time from which vortices are trapped into a pair measured in Fig. 4, and the value corresponding to the second moment behavior from Fig. 16. We see a good agreement with the expected law $\gamma \approx \mu(2) - 1$ (see Table I) [23, 67]. From this observation we can conclude that the superdiffusive behavior of a vortex from the system of 16 vortices is related to the pairing phenomenon. We now shall investigate the

| | 16 vortices | tracers in 4 vortex flow |
|----------|-------------|--------------------------|
| μ | 1.80 | 1.82 |
| γ | 2.68 | 2.82 |

Table I: Trapping times and second moment behavior, for 16 vortices the trapping time is identified with pairing times, while for the tracers the trapping times corresponds to the time spent within a jet (i.e sticky zone). We can notice the very good agreement with the estimate given by $\gamma = 1 + \mu$.

properties of tracers and first start with the chaotic flow generated by four vortices.

C. Passive tracers in 4-vortex system

The results describing the transport properties of passive tracers are illustrated in Fig. 15. We also observe strong anomalous behavior for the tracers with an exponent for the second moment $\mu(2) \approx 1.82$. This behavior was previously observed in [23] for integrable flows driven by three vortices. In this latter case, the origin of the anomalous behavior was directly linked to the presence of islands of regular motion within the stochastic sea and the phenomenon of stickiness observed around them. In the present case the driving flow is chaotic but nevertheless the existence of cores surrounding the vortices and the far field region allows a direct analogy and we may say that the tracer meet similar structures. The only difference is that some of the structure elements (the cores) are “mobile”. Moreover the previous study [23, 25] shows that tracers effectively stick to the vortex cores, and the FTLE field presented in [58] shows that in the far field region the motion of tracers is quasi ballistic, which is a good indication of a sticking behavior.

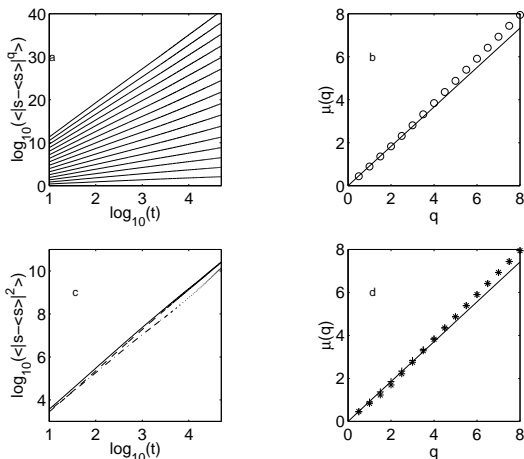


Figure 15: Plot of different transport properties of tracers in 4-vortex system. Plot a, the different moment versus time are plotted for $q = 1/2, 1, \dots, 8$. Plot b, long time exponent behavior for the different moments (see (25)), with $\mu(2) \approx 1.83$ corresponding to a superdiffusive regime. Plot c, second moment versus time, the full line corresponds to the whole data, the dashed line is computed with all trajectories but the parts sticking to vortices, and the dot-dashed line to all trajectories but the part sticking to the outer region. Plot d, different exponents for partial data, * outer region cut ($\mu_f = 1.7$), + vortex-sticking cut ($\mu_s = 1.85$); in both cases the transport is anomalous and superdiffusive.

This conclusion can be strengthened by considering previously described jets. We have seen that the jets are located in the sticky regions, and are either moving around cores and jumping from core to core or rotating

in the far field region. Since we now have “mobile” sticky regions traced by the long lived jets which we are able to monitor, we can estimate that the sticking time (or trapping time in the sticky zone) is more or less similar to the time it takes for a ghost to escape a long lived jet, hence the power law behavior observed in Fig. 7 characterize the exponent γ for trapping time. We then actually observe an exceptional agreement with the expected $\gamma \approx \mu(2) - 1$ relation (see Table I). Hence since the notion of jet as defined in Section IV is relatively general when compared to the notion of core or far field region, we shall say that the anomalous diffusion finds its origin in the existence of long lived “coherent” jets of passive tracers for the chaotic flow generated by four vortices. Since we know that two different types of jets exists (see Fig. 8) and are able to differentiate them easily, in a similar manner as for the three-vortex case [23, 24] we are able to quantify the influence of each type of jet on the transport properties of the system by discarding tracers evolving within a given type of jets. The results of this analysis are presented in Fig. 15, plots c and d. We can conclude that both type of jets are giving rise to anomalous transport with very close characteristic exponents and that they both contribute to the observed strong anomalous diffusion.

D. Passive tracers in 16-vortex system

In both previous cases we observed a signature of anomalous super diffusion with $\mu(2) \approx 1.8$. Let us now investigate the transport properties of passive tracers in a flow generated by 16 identical point vortices, described partially in Section III. there are long lived jets within the region of strong chaos (see Fig. 13) for the flow and the detected jet lives in a vicinity of a vortex and is probably sticking to its core. A snapshot of the system at an early stage is given in Fig. 16 which effectively identifies the cores surrounding the vortices. The results describing the transport properties of passive tracers are in Fig. 17 and show strong anomalous behavior with the exponent $\mu(2) = 1.77$.

Eventhough we only consider one arbitrary initial condition of the vortex system, it is reasonable to assume that the transport properties obtained for such a system are fairly general in the sense that they persist with an increase of the number of vortices if the probability of pairing persists. That means a possibility to neglect the occurrence of more complicated long lived clustering such as the triplet observed in Fig. 2, quadruples, etc...

VI. CONCLUSION AND DISCUSSIONS

In this paper we have investigated the dynamical and statistical properties of the vortex and passive particle advection in chaotic flows generated by four and sixteen point vortices. The goal of the work was to provide qual-

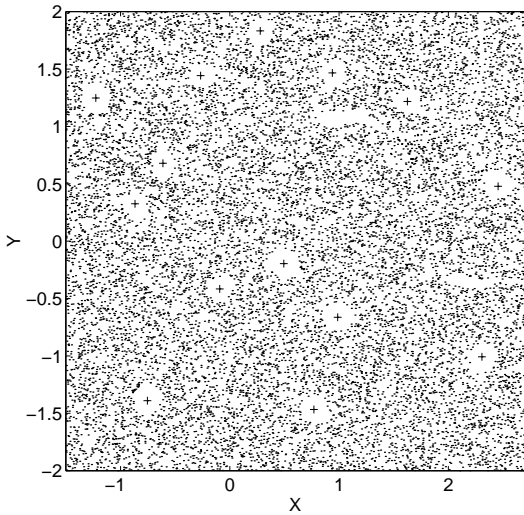


Figure 16: Local snapshot of the system of 16 vortices with $9 \cdot 10^4$ tracers. The vortices are located with the “+” sign. We can see the cores surrounding the vortices. The snapshot is taken early in the simulation to prevent too much dispersion of the tracers and visualize the core. As a consequence we can expect that the actual size of the cores to be a little smaller than the radius of $r \approx 0.1$ one can measure on the snapshot.

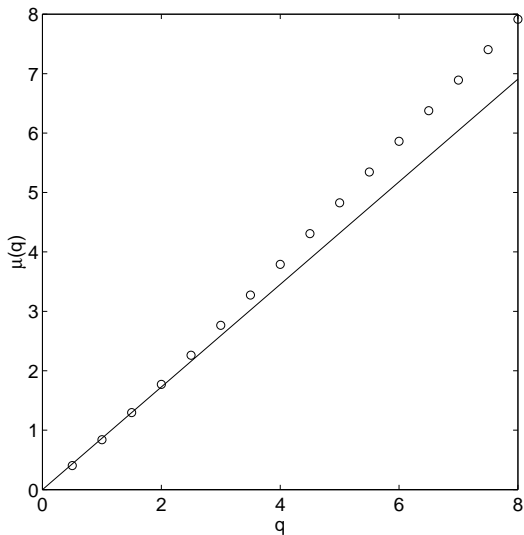


Figure 17: Exponents $\mu(q)$ for the tracer moments for the flow driven by 16 point vortices, with $\mu(2) \approx 1.77$. The slope for small q is 1.75 and for large q is 1.95.

itative insights on general transport properties of two-dimensional flows, especially geophysical ones, imposed by the topology of the phase space. The system of 16 vortices can be considered as a fairly large system while the 4-vortex one is the minimal one with chaotic dynamics of the vortices. The time-averaged spatial distribution of the vortices is characterized by a non-uniform density of vorticity, which implies strong vortex-vortex correlation. These correlations manifest themselves by a phenomenon

of stickiness, namely the formation of long lived pairs of vortices, triplets, etc... Since both these structures are integrable, we can speculate that the stickiness occurs by forming quasi-integrable subsets. The clusters of vortices can form a hierarchical or nested set of integrable subset and hence put some constraints on the frame of possible larger structures involving more vortices. The statistics of pairing time exhibits a power law tail confirming in that way the sticky nature of the phenomenon, which in return allows us to make an analogy with an ideal dynamical system and give a good analytical estimate of the characteristic exponent of the pairing times distribution.

The chaotic nature of the governing flows did not allow the use of diagnostics such as Poincaré maps or distribution of recurrences commonly used for systems with $11/2$ degrees of freedom, hence a new technique inspired by Finite Time Lyapunov Exponents diagnostics has been put into place. Passive tracer motion is analyzed by measuring the mutual relative evolution of two nearby tracers. A possibility of tracers to travel in each other vicinity for relatively large times, confirmed the presence of a hidden order for the tracers which we call jets. The jets can be understood as moving clusters of particles within a specific domain where the motion is almost regular from a coarse grained perspective. The chaotic nature of the motion is confined within the characteristic scale of a given jet, where nearby tracers are trapped. The distribution of trapping times in the jets shows a power-law tail whose characteristic exponent is quantitatively very similar to the one related to pairing times. The calculated Lyapunov exponent for tracers within the jets exponents are similar to what is called Finite Sized Lyapunov Exponent [74], but in our calculations no average is taken and thus a distribution is obtained. These distributions of the Lyapunov exponents exhibit a finite local minimum, which results from the competition of the trapping in jets and the strongly chaotic motion outside the jets. The existence of this minimum allows a dynamical test which identifies if a tracer is trapped within a jet and thus to localize the jet in phase space. Jets are found to exist on the boundary of the cores surrounding the vortices as well as on the outer rim, the region to which vortices have no access to. This behavior is analogous to the sticking one observed in the three vortex case, and thus can be incorporated to the general notion of the phenomenon of stickiness. The differentiation between the two possible types of jets is completely determined by the ratio of the corresponding pair of Lyapunov exponents. We thus obtain de facto a diagnostic to locate coherent structures. The method is then successfully applied to the system of sixteen vortices, leading to a possible general dynamical mechanism of detecting coherent structures. Further analysis of the structure of the jets itself reveals a complicate nested structure of jets within jets, which indicates that jets exists at different scales. The distribution of trapping times within jets is computed and shows a power-law tail whose characteristic exponent is similar to one observed for vortex pairing time.

Since the trapping in jets is also a stickiness phenomenon we may assume that the analytical estimate given for the vortex pairing time is also valid for the trapping time within jets. The transport properties of the 16 vortices as well as those of the tracers in both systems of 4 and 16 vortices are found to be anomalous with characteristic exponent $\mu \sim 1.75 - 1.8$. All these results are in good agreement with the trapping times characteristic exponents and the kinetic theory presented in [23, 24]. Moreover the transport properties are all of the multifractal type or strongly anomalous in the sense defined in [69, 70]. This property of the transport is a conse-

quence of the existence of different sticky zones and the related structures in phase space.

Acknowledgments

The authors would like to express their thanks to L. Kuznetsov for very useful discussions. This work was supported by the U.S. Navy Grants Nos. N00014-96-1-0055 and N00014-97-1-0426, and the U.S. Department of Energy Grant No. DE-FG02-92ER54184.

-
- [1] E. W. Montroll and M. F. Schlesinger, *A wonderful World of Random walk*, in "Studies in Statistical Mechanics", edited by J. Lebowitz and E. W. Montroll (North-Holland, Amsterdam, 1984), vol. 11, p. 1
 - [2] J. P. Bouchaud and A. Georges, Phys. Reports, **95**, 127 (1990)
 - [3] *Levy flights and related topics in Physics*, edited by M. F. Shlesinger, G. M. Zaslavsky and U. Frisch (Springer, Heidelberg, 1995)
 - [4] M. F. Schlesinger, G. M. Zaslavsky and J. Klafter, Nature **363**, 31 (1993)
 - [5] G. Zimbardo, P. Veltri and P. Pommois, *anomalous, quasilinear, and percolative regimes for magnetic field line transport in axially symmetric turbulence*, Phys. Rev E, **61**, 1940 (2000)
 - [6] G. Zimbardo, A. Greco and P. Veltri, *Superballistic transport in tearing driven magnetic turbulence*, Phys. Plasmas **7**, 1071 (2000)
 - [7] G. Manfredi, C. M. Roach and R. O. Dendy, *Zonal flow and streamer generation in drift turbulence*, Plasma Phys. Control. Fusion **43**, 825 (2001)
 - [8] S. V. Annibaldi, G. Manfredi, R. O. Dendy and L. O'C Drury, *Evidence for strange kinetics in Hasegawa-Mima turbulent transport*, Plasma Phys. Control. Fusion **42**, L13 (2000)
 - [9] A. A. Chernikov, B. A. Petrovichev, A. V. Rogal'sky, R. Z. Sagdeev, and G. M. Zaslavsky, *Anomalous Transport of Streamlines Due to their Chaos and their Spatial Topology*, Phys. Lett. A **144**, 127 (1990)
 - [10] T.H. Solomon, E.R. Weeks, H.L. Swinney, *Chaotic advection in a two-dimensional flow: Lévy flights in and anomalous diffusion*, Physica D, **76**, 70 (1994)
 - [11] E.R. Weeks, J.S. Urbach, H.L. Swinney, *Anomalous diffusion in asymmetric random walks with a quasi-geostrophic flow example*, Physica D, **97**, 219 (1996)
 - [12] G.M. Zaslavsky, D. Stevens, H. Weitzner, *Self-similar transport in incomplete chaos*, Phys. Rev E **48**, 1683 (1993)
 - [13] S. Kovalyov, *Phase space structure and anomalous diffusion in a rotational fluid experiment*, Chaos **10**, 153 (2000)
 - [14] A. Provenzale, *Transport by Coherent Barotropic Vortices*, Annu. Rev. Fluid Mech. **31**, 55 (1999)
 - [15] A. J. Majda, J. P. Kramer, *Simplified models for turbulent diffusion: Theory, numerical modeling, and physical phenomena*, Phys. Rep. **314**, 238 (1999)
 - [16] J. B. Weiss, A. Provenzale, J. C. McWilliams, *Lagrangian dynamics in high-dimensional point-vortex system*, Phys. Fluids **10**, 1929 (1998)
 - [17] P. Tabeling, A.E. Hansen, J. Paret, *Forced and Decaying 2D turbulence: Experimental Study*, in "Chaos, Kinetics and Nonlinear Dynamics in Fluids and Plasma", eds. Sadruddin Benkadda and George Zaslavsky, p. 145, (Springer 1998)
 - [18] A. E Hansen, D. Marteau, P. Tabeling, *Two-dimensional turbulence and dispersion in a freely decaying system*, Phys. Rev. E **58**, 7261 (1998)
 - [19] P. Tabeling, S. Burkhart, O. Cardoso, H. Willaime, *Experimental-Study of Freely Decaying 2-Dimensional Turbulence*, Phys. Rev. Lett. **67**, 3772 (1991)
 - [20] V.V. Meleshko, M.Yu. Konstantinov, *Vortex Dynamics and Chaotic Phenomena*, (World Scientific, Singapore, 1999)
 - [21] L. Kuznetsov and G.M. Zaslavsky, *Regular and Chaotic advection in the flow field of a three-vortex system*, Phys. Rev E **58**, 7330 (1998).
 - [22] Z. Neufeld and T. Tél, *The vortex dynamics analogue of the restricted three-body problem: advection in the field of three identical point vortices*, J. Phys. A: Math. Gen. **30**, 2263 (1997)
 - [23] L. Kuznetsov and G. M. Zaslavsky, *Passive particle transport in three-vortex flow*. Phys. Rev. E. **61**, 3777 (2000).
 - [24] X. Leoncini, L. Kuznetsov and G. M. Zaslavsky, *Chaotic advection near 3-vortex Collapse*, Phys. Rev.E, **63**, 036224-1 (2001)
 - [25] A. Laforgia, X. Leoncini, L. Kuznetsov and G. M. Zaslavsky, Eur. Phys. J. B, **20**, 427 (2001)
 - [26] H.Aref, *Stirring by chaotic advection*, J. Fluid Mech. **143**, 1 (1984)
 - [27] G. M. Zaslavsky, R. Z. Sagdeev, and A. A. Chernikov, Zhurn. Eksp. Teor. Fiz. **94**, 102 (1988) (Soviet Physics, JETP **67**, 270 (1988))
 - [28] J. Ottino, *The kinematics of Mixing: Stretching, Chaos, and Transport* (Cambridge U. P., Cambridge, 1989)
 - [29] H.Aref, *Chaotic advection of fluid particles*, Phil. Trans. R. Soc. London **A 333**, 273 (1990)
 - [30] J. Ottino, *Mixing, Chaotic advection and turbulence*, Ann. Rev. Fluid Mech. **22**, 207 (1990)
 - [31] V. Rom-Kedar, A. Leonard and S. Wiggins, *An analytical study of transport mixing and chaos in an unsteady vortical flow*, J. Fluid Mech. **214**, 347 (1990)
 - [32] G. M. Zaslavsky, R. Z. Sagdeev, D. A. Usikov, and A.

- A. Chernikov, *Weak Chaos and Quasiregular Patterns*, Cambridge Univ. Press, (Cambridge 1991)
- [33] A. Crisanti, M. Falcioni, G. Paladin and A. Vulpiani, *Lagrangian Chaos: Transport, Mixing and Diffusion in Fluids*, La Rivista del Nuovo Cimento, **14**, 1 (1991)
- [34] A. Crisanti, M. Falcioni, A. Provenzale, P. Tanga and A. Vulpiani, *Dynamics of passively advected impurities in simple two-dimensional flow models*, Phys. Fluids A **4**, 1805 (1992)
- [35] R. Benzi, G. Paladin, S. Patarnello, P. Santangelo and A. Vulpiani, *Intermittency and coherent structures in two-dimensional turbulence*, J. Phys A **19**, 3771 (1986)
- [36] R. Benzi, S. Patarnello and P. Santangelo, *Self-similar coherent structures in two-dimensional decaying turbulence*, J. Phys A **21**, 1221 (1988)
- [37] J. B. Weiss, J. C. McWilliams, *Temporal scaling behavior of decaying two-dimensional turbulence*, Phys. Fluids A **5**, 608 (1992)
- [38] J. C. McWilliams, *The emergence of isolated coherent vortices in turbulent flow*, J. Fluid Mech. **146**, 21 (1984)
- [39] J. C. McWilliams, *The vortices of two-dimensional turbulence*, J. Fluid Mech. **219**, 361 (1990)
- [40] D. Elhmaïdi, A. Provenzale and A. Babiano, *Elementary topology of two-dimensional turbulence from a Lagrangian viewpoint and single particle dispersion*, J. Fluid Mech. **257**, 533 (1993)
- [41] G. F. Carnevale, J. C. McWilliams, Y. Pomeau, J. B. Weiss and W. R. Young, *Evolution of Vortex Statistics in Two-Dimensional Turbulence*, Phys. Rev. Lett. **66**, 2735 (1991)
- [42] N. J. Zabusky, J. C. McWilliams, *A modulated point-vortex model for geostrophic, β -plane dynamics*, Phys. Fluids **25**, 2175 (1982)
- [43] P. W. C. Vobseck, J. H. G. M. van Geffen, V. V. Meleshko, G. J. F. van Heijst, *Collapse interaction of finite-sized two-dimensional vortices*, Phys. Fluids **9**, 3315 (1997)
- [44] O. U. Velasco Fuentes, G. J. F. van Heijst, N. P. M. van Lipzig, *Unsteady behaviour of a topography-modulated tripole*, J. Fluid Mech. **307**, 11 (1996)
- [45] R. Benzi, M. Colella, M. Briscolini, and P. Santangelo, *A simple point vortex model for two-dimensional decaying turbulence*, Phys. Fluids A **4**, 1036 (1992)
- [46] J. B. Weiss, *Punctuated Hamiltonian Models of Structured Turbulence*, in *Semi-Analytic Methods for the Navier-Stokes Equations*, CRM Proc. Lecture Notes, **20**, 109, (1999)
- [47] O. Agullo and A. D. Verga Phys. Rev E **63**, 056304 (2001)
- [48] H. Aref, *Motion of three vortices*, Phys. Fluids **22**, 393 (1979)
- [49] H. Aref, *Integrable, chaotic and turbulent vortex motion in two-dimensional flows*, Ann. Rev. Fluid Mech. **15**, 345 (1983)
- [50] E. A. Novikov, *Dynamics and statistics of a system of vortices*, Sov. Phys. JETP **41**, 937 (1975)
- [51] J. L. Synge, *On the motion of three vortices*, Can. J. Math. **1**, 257 (1949)
- [52] X. Leoncini, L. Kuznetsov and G. M. Zaslavsky, *Motion of Three Vortices near Collapse*, Phys. Fluids **12**, 1911 (2000)
- [53] J. Tavantzis and L. Ting, *The dynamics of three vortices revisited*, Phys. Fluids **31**, 1392 (1988)
- [54] E. A. Novikov, Yu. B. Sedov, Stochastic properties of a four-vortex system, Sov. Phys. JETP **48**, 440 (1978)
- [55] H. Aref and N. Pomphrey, *Integrable and chaotic motions of four vortices: I. the case of identical vortices*, Proc. R. Soc. Lond. A **380**, 359 (1982).
- [56] S. L. Ziglin, *Nonintegrability of a problem on the motion of four point vortices*, Sov. Math. Dokl. **21**, 296 (1980)
- [57] A. Babiano, G. Boffetta, A. Provenzale and A. Vulpiani, *Chaotic advection in point vortex models and two-dimensional turbulence*, Phys. Fluids **6**, 2465 (1994)
- [58] S. Boatto and R. T. Pierrehumbert, *Dynamics of a passive tracer in a velocity field of four identical point vortices*. J. Fluid Mech. **394**, 137 (1999).
- [59] V. V. Afanasiev, R. Z. Sagdeev, and G. M. Zaslavsky, *Chaos* **1**, 143 (1991)
- [60] H. Lamb, *Hydrodynamics*, (6th ed. New York, Dover, 1945).
- [61] R.I. McLachlan, P. Atela, *The accuracy of symplectic integrators*, Nonlinearity **5**, 541 (1992).
- [62] E. Ott, *Dynamic Chaos* (Cambridge Univ. Press, Cambridge, 1998)
- [63] V. K. Melnikov, *On the existence of self-similar structures in the resonance domain*, in *Transport, Chaos and Plasma Physics II, Proceedings, Marseille*, edited by F. Doveil, S. Benkadda, and Y. Elskens (World Scientific, Singapore, 1996), pp. 142-153
- [64] V. Rom-Kedar and G. M. Zaslavsky, *Islands of accelerator modes and homoclinic tangles*, Chaos **9**, 697 (1999)
- [65] V.V. Meleshko, M.Yu. Konstantinov, *Vortex Dynamics and Chaotic Phenomena*, (World Scientific, Singapore, 1999) **7**, 159 (1997)
- [66] G. M. Zaslavsky, M. Edelman, B. A. Niyazov, *Self-similarity, renormalization, and phase space nonuniformity of Hamiltonian chaotic dynamics*, Chaos **7**, 159 (1997)
- [67] G. M. Zaslavsky and M. Edelman, *Hierarchical structures in the phase space and fractional kinetics: I. Classical systems*, Chaos **10**, 135 (2000)
- [68] G. Haller and G. Yuan, *Lagrangian coherent structures and mixing in two-dimensional turbulence*, Preprint (2000)
- [69] P. Castiglione, A. Mazzino, P. Mutatore-Ginanneschi, A. Vulpiani, *On Strong anomalous diffusion*, Physica D, **134**, 75 (1999)
- [70] K. H. Andersen, P. Castiglione, A. Massino, A. Vulpiani, *Simple stochastic models showing strong anomalous diffusion*, Eur. Phys. J. B, **18**, 447 (2000)
- [71] E. Aurell, G. Boffetta, A. Crisanti, G. Paladin and A. Vulpiani, *Predictability in the large: an extension of the concept of Lyapunov exponent*, J. Phys. A, **30**, 1 (1997)
- [72] S. Benkadda, S. Kassibrakis, R. White and G. M. Zaslavsky, Phys. Rev. E, **59**, 3761 (1999)
- [73] H. Weitzner and G. M. Zaslavsky, *Directional fractional Kinetics*, Chaos **11**, 384 (2001)
- [74] R. Ferrari, A. J. Manfroi, W. R. Young, *Strong and weakly self-similar diffusion*, Physica D, **154**, 111 (2001)
- [75] G. M. Zaslavsky, *Multifractional kinetics*, Physica A, **288**, 431 (2000)
- [76] G. M. Zaslavsky, *Fractional Kinetics of Hamiltonian Chaotic Systems*, in "Application of fractional Calculus in Physics", Ed. R. Hilfer (World Scientific, Singapore, 2000), p. 203